Performance of GaAs MESFET Mixers at *X* Band

ROBERT A. PUCEL, SENIOR MEMBER, IEEE, DANIEL MASSÉ, MEMBER, IEEE, AND RICHARD BERA

Abstract—**A theoretical analysis and experimental verification of the signal properties of the GaAs MESFET mixer are presented. Experimental techniques for evaluating some of the mixer parameters are described.**

Experiments performed on GaAs MESFET mixers at *X* band show that good noise performance and large dynamic range can be achieved with conversion gain. A conversion gain over 6 dB is measured at 7.8 GHz. Noise figures as low as 7.4 dB and output third-order intermodulation intercepts of +18 dBm have been obtained at 8 GHz with a balanced MESFET mixer.

I. Introduction

THE low-noise performance of GaAs Schottky barrier gate field-effect transistors (MESFET's) as high-gain linear amplifiers in the high microwave band (*C*–*X* band) has been demonstrated by many laboratories [1].[1] In this paper we shall show that these transistors also have the potential for low-noise operation as microwave mixers with gain and high dynamic range. As such, they combine the best features of the tunnel diode and the Schottky barrier diode mixer.

We also show in this paper how certain of the FET mixer parameters can be measured. Using the measured parameter values in the theory developed here, we obtain good agreement with experiment.

Our experiments were performed at *X* band with single-gate GaAs MESFET's. These studies, a natural extension of our investigations of the GaAs FET linear amplifier, were intended to assess the suitability of the GaAs FET as a building block for the three basic active components of an integrated front end at *X* band, namely the RF amplifier, local oscillator, and mixer. The devices used in the mixer studies were the same as those used in the low-noise amplifier experiments. That is to say, no attempt was made to optimize them for mixer applications.

II. Frequency Conversion in an FET

The small-signal equivalent circuit of the unpackaged FET valid at frequencies up to *X* band and higher is illustrated in Fig. 1. Additional parasitic elements, such as lead inductances and interelectrode capacitances, must be added for a device mounted in a package. (Our experiments were made with unpackaged FET's with beam leads.) In a well-designed GaAs MESFET the parasitic contact resistances R_{gm}, R_s, and R_{dr} in the gate, source, and drain leads, respectively, are small compared to the drain resistance R_d.

Manuscript received October 3, 1975; revised December 17, 1975.
The authors are with the Research Division, the Raytheon Company, Waltham, MA 02154.

[1] Since in this paper we shall consider only GaAs Schottky barrier gate field-effect transistors, we use the terms GaAs MESFET, GaAs FET, and FET interchangeably.

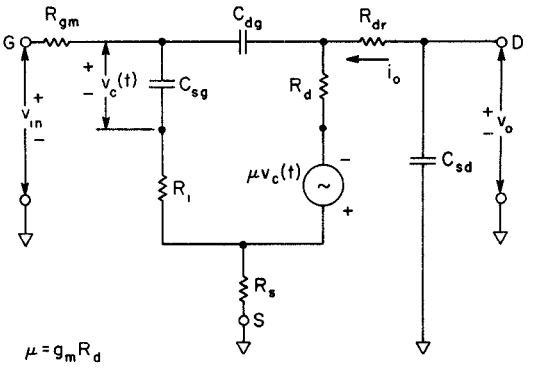

Fig. 1. Small-signal equivalent circuit of the GaAs field-effect transistor.

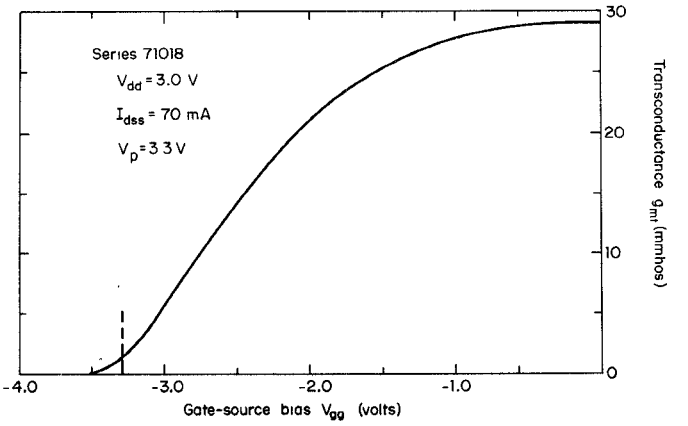

Fig. 2. Measured terminal transconductance as a function of gate bias of a GaAs MESFET used in mixer experiments.

However, R_{gm} and R_s are the principal sources of extrinsic noise [2].

Mixing occurs in an FET when the small-signal elements representing the FET are varied at a periodic rate by a large local oscillator signal impressed between a pair of the device terminals, usually the gate-source terminals. In a GaAs MESFET the strongest gate-bias dependence is exhibited by the transconductance g_m. The mixing products attributable to parametric "pumping" of the source-gate capacitance C_{sg} and its charging resistance R_i are negligible. The drain resistance also shows a strong gate-bias dependence. However, since it is not integral to the gain mechanism of the FET, we have used only its time-averaged value in our theory. The theory can be generalized to remove this simplification, but our experimental results did not require this, at least for the signal properties of the mixer.

Fig. 2 is a graph of the measured transconductance of a

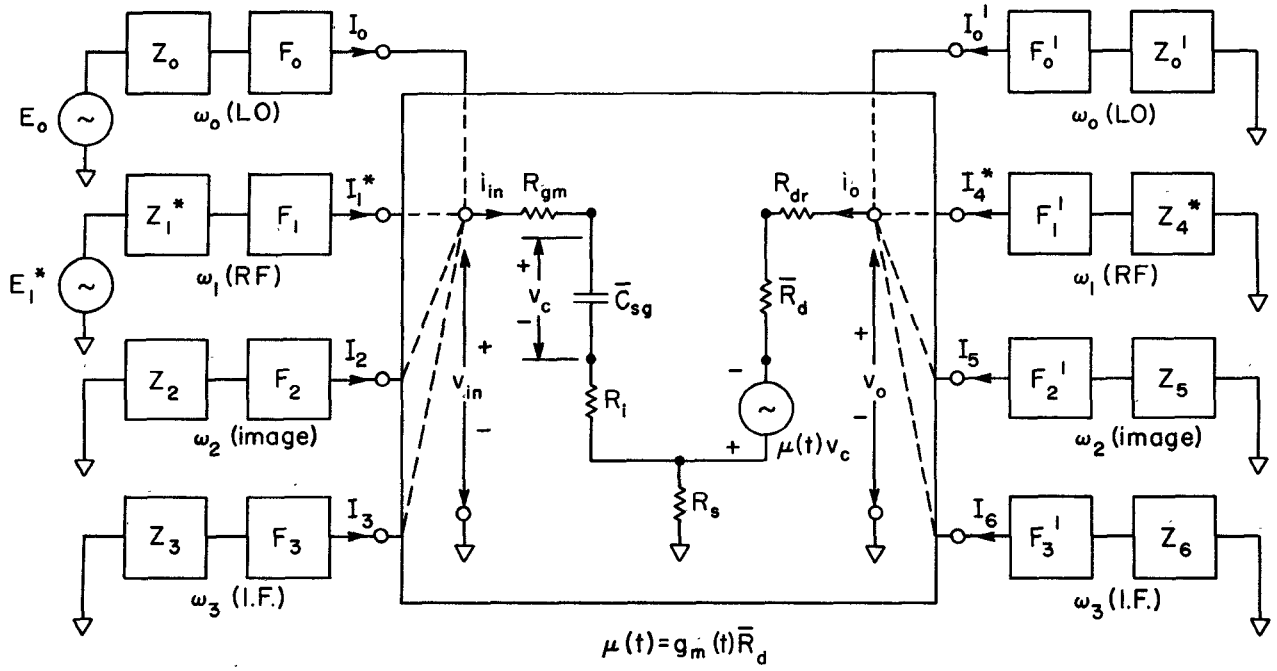

Fig. 3. Schematic of FET mixer, including signal, image, and IF circuits, used in signal analysis.

typical microwave FET as a function of the potential difference V_{gg} between the gate and source terminals when the drain-source bias voltage V_{dd} has a value somewhere above the knee of the I–V characteristic, in this case 3.0 V. The functional dependence for any other value of drain voltage above the knee is similar.

Assume that for a fixed value of gate-source bias, a large LO signal is superimposed on the gate-source terminals. The transconductance becomes a time-varying function $g_m(t)$ with a period equal to that of the LO. If ω_0 denotes the oscillator frequency, we may write

$$g_m(t) = \sum_{k=-\infty}^{\infty} g_k e^{jk\omega_0 t} \tag{1}$$

where

$$g_k = \frac{1}{2\pi}\int_0^{2\pi} g(t)e^{-jk\omega_0 t}d(\omega_0 t). \tag{2}$$

All harmonic amplitudes can be assumed to be real by proper choice of the time reference. In accordance with our earlier stated assumption, we will neglect all harmonic components of $R_d(t)$, so that the time-varying voltage amplification factor $\mu(t)$ can be written as $\mu(t) \approx \bar{R}_d g_m(t)$, where $\bar{R}_d = R_0$ is the time-averaged component of the drain resistance.

Let a small-signal $v_c(t)$ of frequency $\omega_1 \neq \omega_0$ be impressed on the gate capacitance, as indicated in Fig. 1. By the mixing action of the time-varying transconductance, a voltage $\mu(t)v_c(t)$ is generated in the drain circuit. This signal has side-band frequency components $|n\omega_0 \pm \omega_1|$, where n takes on all integer values.

An analysis of a practical FET mixer must include side-band components in both the gate (input) and drain (output) circuits. In our analysis we shall focus attention on the down-converter, where the output or intermediate (IF) frequency $\omega_3 = |\omega_0 - \omega_1|$ is less than the signal frequency ω_1. Then the only remaining frequency component of first-order importance is the image frequency ω_2, where $|\omega_2 - \omega_1| = 2\omega_3$. For convenience we shall assume $\omega_1 < \omega_0 < \omega_2$.

Let V_1, V_2, V_3 and I_1, I_2, I_3 represent the complex voltage and current amplitudes of the signal, image, and IF components in the gate circuit, and V_4, V_5, V_6 and I_4, I_5, I_6 the corresponding voltage and current amplitudes, respectively, of the components in the drain circuit. Suppose the input signal at ω_1 is driven by a voltage source E_1 of internal impedance Z_1 and all other side-band components, including the desired output signal at frequency ω_3, are terminated in complex impedances. Then the boundary conditions at the gate source and drain-source terminals, relating the voltage and current amplitudes V_k and I_k are

$$V_k = E_k - I_k Z_k, \qquad (k = 1,2,\cdots,6) \tag{3}$$

where $E_k = 0$ for $k \neq 1$.

The equivalent circuit of the FET mixer, based on Fig. 1, representing (3) is shown in Fig. 3. Because we have chosen the incoming signal frequency to be the "lower side band," i.e., $\omega_1 < \omega_0$, we must use the complex conjugate component of the signal. This will be denoted by the asterisk (*). In our representation the boxes labeled F_k and F_k' are fictitious ideal (lossless) filters which have zero impedance at the desired frequency and infinite impedance at all the remaining side-band components. In practice, of course, these filters are not ideal and are not necessarily separable in a physical sense. Neither are the set of input ports, or output ports, physically separable. The source-drain capacitance does not appear in Fig. 3 since we have included it as part of the filter-termination circuit of each output port.

We have also included a set of input and output oscillator ports. The oscillator signal is assumed to be injected at the gate terminal as shown in Fig. 3. It could also be inserted in series with the source terminal, but this is not a convenient method at high frequencies. The oscillator port at the output is necessary because a large current component at this frequency is generated by the "pumping" of the drain current. This port is usually terminated in a low impedance, for example, a short-circuiting transmission line stub. When the IF is low, the output termination for the oscillator, signal, and image components can be the same circuit element.

III. Circuit Analysis

A. Signal Equations

The linear circuit relations between the various frequency components can be derived by a loop analysis of Fig. 3. In matrix notation these equations are written as

$$[E] = [V] + [Z_t][I] \tag{4a}$$

$$= [Z_m][I] + [Z_t][I] \tag{4b}$$

where

$$[E] = \begin{bmatrix} E_1^* \\ 0 \\ 0 \\ 0 \\ 0 \\ 0 \end{bmatrix} \quad [V] = \begin{bmatrix} V_1^* \\ V_2 \\ V_3 \\ V_4^* \\ V_5 \\ V_6 \end{bmatrix} \quad [I] = \begin{bmatrix} I_1^* \\ I_2 \\ I_3 \\ I_4^* \\ I_5 \\ I_6 \end{bmatrix}$$

and $[Z_m]$ and $[Z_t]$ are, respectively, the matrices representing the mixer proper and its terminations. These are given by

$$[Z_m] = \begin{bmatrix} Z_{11}^* & 0 & 0 & Z_{14}^* & 0 & 0 \\ 0 & Z_{22} & 0 & 0 & Z_{25} & 0 \\ 0 & 0 & Z_{33} & 0 & 0 & Z_{36} \\ Z_{41}^* & 0 & Z_{43} & Z_{44}^* & 0 & 0 \\ 0 & Z_{52} & Z_{53} & 0 & Z_{55} & 0 \\ Z_{61}^* & Z_{62} & Z_{63} & 0 & 0 & Z_{66} \end{bmatrix}$$

$$[Z_t] = \begin{bmatrix} Z_1^* & 0 & 0 & \cdot & \cdot & \cdot \\ 0 & Z_2 & & & & \\ 0 & & Z_3 & & & \\ \cdot & & & Z_4^* & & \\ \cdot & & & & Z_5 & \\ \cdot & & & & & Z_6 \end{bmatrix}.$$

If we neglect mixing by harmonics of $g_m(t)$ higher than the first, the matrix elements are

$$Z_{kk}(\omega_k) = R_{gm} + R_i + R_s + \frac{1}{j\omega_k \bar{C}}, \quad (k = 1,2,3)$$

$$= R_{dr} + \bar{R}_d + R_s, \quad (k = 4,5,6) \tag{5a}$$

$$Z_{14} = Z_{25} = Z_{36} = R_s \tag{5b}$$

$$Z_{41} = \frac{-g_0\bar{R}_d}{j\omega_1\bar{C}} + R_s \qquad Z_{61} = \frac{-g_1\bar{R}_d}{j\omega_1\bar{C}}$$

$$Z_{52} = \frac{-g_0\bar{R}_d}{j\omega_2\bar{C}} + R_s \qquad Z_{62} = \frac{-g_1\bar{R}_d}{j\omega_2\bar{C}}$$

$$Z_{63} = \frac{-g_0\bar{R}_d}{j\omega_3\bar{C}} + R_s \qquad Z_{43} = Z_{53} = \frac{-g_1\bar{R}_d}{j\omega_3\bar{C}}. \tag{5c}$$

Here $\bar{C}$ represents the time-averaged value of the source-gate capacitance.

B. Conversion Gain

The available conversion gain G_{av} between the RF input, port 1, and the IF output, port 6, is expressible as

$$G_{av} = \frac{|I_6|^2 \operatorname{Re} Z_6}{|E_1|^2/4 \operatorname{Re} Z_1} \tag{6a}$$

$$= 4R_gR_L \left|\frac{I_6}{E_1}\right|^2 \tag{6b}$$

where the source and load impedances are defined, respectively, as $Z_1 \equiv Z_g = R_g + jX_g$ and $Z_6 \equiv Z_L = R_L + jX_L$. The ratio I_6/E_1 is obtained from the solution of (4). If we let Δ_z denote the determinant of the matrix $[Z_m] + [Z_t]$, and Δ the determinant of the matrix obtained by deletion of the first row and sixth column, then $I_6/E_1 = -\Delta/\Delta_z$.

The expression for G_{av} is a complicated function of the terminations on each port. The derivation is given in the Appendix. However, when the intermediate frequency is small compared to the input signal frequency, drastic simplifications are introduced. Not only does the image at the input side "see" the same termination as the source, but the gain becomes insensitive to the IF termination at the input side and the image and RF terminations at the output side. We have verified this insensitivity to terminations in our experiments since our IF was 30 MHz and the RF was 8 GHz.

We find from the Appendix that the gain expression for this case simplifies to

$$G_{av} = \left(\frac{2g_1\bar{R}_d}{\omega_1\bar{C}}\right)^2 \frac{R_g}{(R_g + R_{in})^2 + \left(X_g - \frac{1}{\omega_1\bar{C}}\right)^2} \cdot \frac{R_L}{(\bar{R}_d + R_L)^2 + X_L^2} \tag{7}$$

where $R_{in} = R_{gm} + R_i + R_s$ is the input resistance. Note that the gain has a bandpass shape factor for the input and output circuits, as one might expect. The gain is maximum at band center when the source and load are conjugately matched to the FET, that is, for $R_g = R_{in}$, $X_g = (\omega_1\bar{C})^{-1}$; $R_L = \bar{R}_d$, $X_L = 0$. Defining $G_c = G_{av,\,max}$, we find

$$G_c = \frac{g_1^2}{4\omega_1^2\bar{C}^2}\frac{\bar{R}_d}{R_{in}}. \tag{8}$$

We shall hereafter refer to the maximum available mixer gain as the conversion gain.

It is not surprising that this expression for conversion gain is of the same form as that for the maximum available

amplifier gain G_a

$$G_a = \frac{g_m^2}{4\omega_1^2 C^2} \frac{R_d}{R_{in}} \tag{9}$$

where the time-averaged quantities g_1, $\bar{C}$, and $\bar{R}_d$ are replaced by the values pertaining to a specific bias condition. The ratio of these two gains, corresponding to the same signal input frequency,

$$\frac{G_c}{G_a} = \left(\frac{g_1}{g_m}\right)^2 \left(\frac{C}{\bar{C}}\right)^2 \frac{\bar{R}_d}{R_d} \tag{10}$$

can be larger than unity. That is, the conversion gain can exceed the amplifier gain. We shall demonstrate this later. Even though $g_1/g_m < 1$, the ratios $C/\bar{C}$ and $\bar{R}_d/R_d$ are greater than unity since for maximum conversion gain the device is biased near pinchoff, in contrast to the amplifier for which the gate is operated at or near zero bias.

C. Bias Dependence of Mixer Gain Parameters

The conversion gain is a strong function of the gate bias and LO drive. The quantity most strongly dependent is the conversion conductance g_1. One might expect g_1 to be greatest for a gate bias near pinchoff, since it is here that the transconductance is most sensitive to bias modulation by the LO. This is true. To demonstrate this, let the instantaneous voltage between the gate-source terminals be represented as

$$V_{sg}(t) = V_{gg} + V_0 \cos \omega_0 t \tag{11}$$

where V_{gg} is the dc bias and V_0 the peak RF amplitude of the LO drive. This modulation wave is shown in the inset of Fig. 4(a).

Also illustrated in this figure is a plot of the theoretical conversion conductance as a function of dc bias when the LO amplitude is chosen to be the maximum possible value. This is taken to correspond to the onset of forward conduction of the Schottky barrier gate (approximately 0.5-V forward bias). Excessive forward conduction requires unnecessary LO power. The curve was calculated by a numerical Fourier analysis of $g_m(t)$ for the experimental curve shown in Fig. 2. Notice that a broad maximum in the curve occurs at approximately $V_{gg} = -3.2$ V, near the pinchoff point for g_m (Fig. 2).

Observe from Figs. 2 and 4(a) that the maximum value of g_1 is approximately one-third of the maximum (zero-bias) value of g_m. This ratio is close to the $1/\pi$ ratio obtained for the "ideal" case when g_m is a step function of gate bias.

For LO drive amplitudes below the maximum level, curves similar to Fig. 4(a) would be obtained, but of progressively lower value. We show this dependence explicitly for the gate bias corresponding to pinchoff [Fig. 4(b)]. The steeper the g_m curve is near pinchoff, the steeper the g_1 curve is near zero LO drive. In fact, for an ideal g_m versus V_{gg} dependence, the g_1 curve in Fig. 4(b) would also be a step function, with maximum g_1 occurring for vanishing LO drive.

Gate capacitance exhibits a much milder dependence on gate bias. The experimental points in Fig. 5 were obtained for the same FET whose transconductance curves were shown previously. Beyond the pinchoff bias, C_{sg} continues to decrease. Because of the mild variation of C_{sg}, we have approximated the experimental data by a linear function of bias, as shown by the solid line. For other devices, quadratic and higher order terms may be needed.

In general, if the gate bias dependence of C_{sg} is highly nonlinear, the average capacitance $\bar{C}$ "seen" by the small signals differs from the average capacitance $\bar{C}_0$ "seen" by

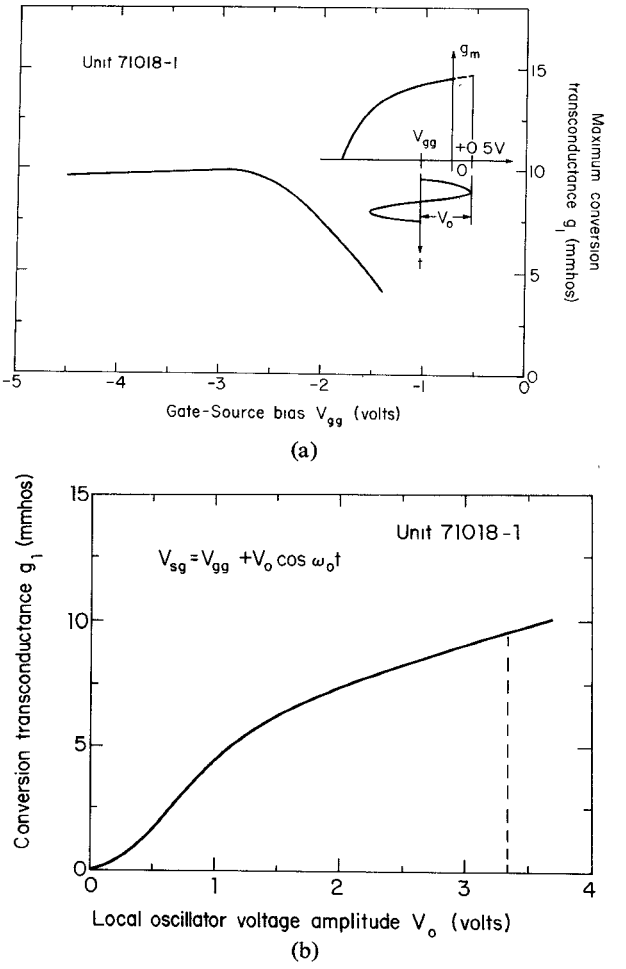

Fig. 4. Calculated (a) conversion transconductance at maximum LO drive as a function of gate bias and (b) conversion transconductance at pinchoff bias as a function of LO drive.

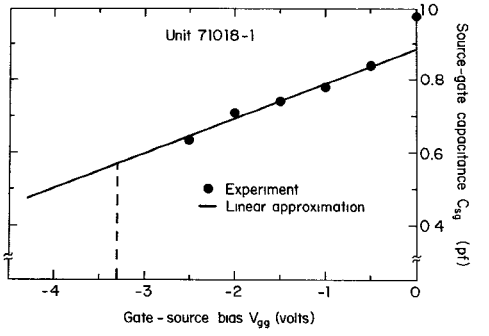

Fig. 5. Measured source-gate capacitance as a function of gate bias and its linear approximation.

the LO, and both differ from the static value at the bias point $C_{sg} = C_{sg}(V_{gg})$. When a linear approximation to the $C_{sg}(V_{gg})$ data is possible, as in Fig. 5, all three capacitance values coincide, $\bar{C} = \bar{C}_0 = C_{sg}(V_{gg})$. For the nonlinearities we have observed in microwave GaAs MESFET's, the linear approximation seems adequate in most cases.

D. Experimental Determination of Mixer Parameters

If one wishes to predict the conversion gain at some LO power and gate bias, or to compare the measured gain with the predicted value, it is necessary to know the amplitude of the LO voltage across the gate capacitance. Then g_1 and $\bar{R}_d$ can be calculated by a Fourier analysis of the time-varying drain resistance and transconductance. Therefore an experimental determination of the oscillator voltage amplitude V_0 is necessary.

There are several schemes for deducing V_0. One method is based on the formula for the LO power P_0 dissipated in the gate circuit

$$P_0 = \tfrac{1}{2}(\omega_0 \bar{C}_0 V_0)^2 R_{in} \tag{12}$$

where $R_{in} = R_{gm} + R_i + R_s$ is the input resistance as defined earlier. If $\bar{C}_0$ can be assumed reasonably insensitive to LO drive, as discussed earlier, and if R_{in} is known from small-signal scattering parameter measurements, then V_0 is easily determined from (12). It is important that P_0 be corrected for circuit losses.

Another method makes use of the measurable shift in the average drain current when a large signal is impressed on the gate. If a piecewise linear approximation to the $I_d - V_{sg}$ characteristic is permissible, as sketched in the inset of Fig. 6, then when biased at pinchoff, the shift in average drain current is linearly related to the oscillator voltage

$$\Delta \bar{I}_d = \frac{I_{dss}}{\pi} \frac{V_0}{V_p} \tag{13}$$

where I_{dss} is the zero bias drain current and V_p is the magnitude of the gate bias for current pinchoff. Since I_{dss} and V_p are measurable, V_0 can be determined from (13). It is important in the experiment that the drain circuit present a low impedance at the oscillator frequency and its first few harmonics, otherwise the waveform of the time-varying drain current will be distorted.

When (13) is valid, and if a straight-line approximation of the $C_{sg}(V_{sg})$ data is permissible, $\Delta \bar{I}_d$ is a linear function of $\sqrt{P_0}$ by virtue of (12). The data in Fig. 6 are an example of this linear relationship. The slope of the line

$$S = \frac{1}{\pi} \frac{I_{dss}}{V_p} \sqrt{\frac{2}{\omega_0^2 \bar{C}_0^2 R_{in}}} \tag{14}$$

allows one to determine the product $\bar{C}_0^2 R_{in}$ without knowledge of R_{in}. If $\bar{C}_0$ is known from capacitance data, one may determine R_{in} without recourse to high-frequency small-signal measurements. Furthermore, since $\bar{C} \approx \bar{C}_0$, this R–C product can be inserted directly into the denominator of the conversion gain expression (8).

The determination of $\bar{R}_d$ by Fourier analysis is not recommended since the low-frequency drain resistance often shows an erratic dependence on gate bias which is not evident at higher frequencies. It is preferable to obtain $\bar{R}_d$ by measurement of the resistance presented to the FET by the IF circuit when the IF load is adjusted for maximum conversion gain at each LO drive. This was the method used by us.

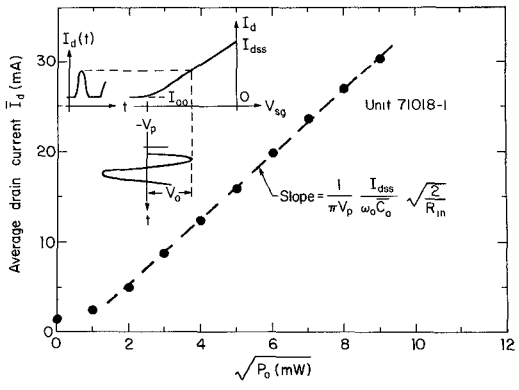

Fig. 6. Increase in average drain current as a function of LO drive when FET is biased near pinchoff.

E. Noise

Noise in a microwave FET is produced by sources intrinsic to the device; by thermal sources associated with the parasitic resistances, i.e., the gate metallization and source and drain contact resistances, and by extraneous sources arising from defects in the semiconductor material such as traps. The spectrum of the instrinsic and thermal sources is "flat," i.e., white noise, extending well beyond the microwave band. The trap noise, generally, shows a rapid drop with frequency, often exhibiting a $1/f$-like character. As such it is more pronounced in the IF frequency band than in the signal band.

Experiments performed at this laboratory show that the $1/f$ component of the noise spectrum in the drain current extends at least up to 100 MHz. The experimental results reported here give evidence that the $1/f$ noise may be responsible for the degradation of the mixer noise performance at the 30 MHz IF.

The theoretical analysis of noise in a GaAs MESFET mixer is complicated because the correlation between the instrinsic drain noise and the induced gate noise cannot be neglected and is also a time-varying function. An analysis of the noise performance of a GaAs MESFET mixer is in progress.

IV. Experimental Results

A. Introduction

In this section we shall describe experimental results obtained with two different series of GaAs MESFET's. The first FET, series 71018, has a gate length of approximately 2.5 μm, a gate width of 500 μm, a terminal pinchoff voltage $V_p \approx 3.3$ V,[2] and a channel doping of 8×10^{16} cm^{-3}.

[2] By terminal pinchoff we mean the intrinsic pinchoff voltage W_{oo} less the built-in barrier potential ϕ of the gate, where $\phi \approx 0.9$ V.

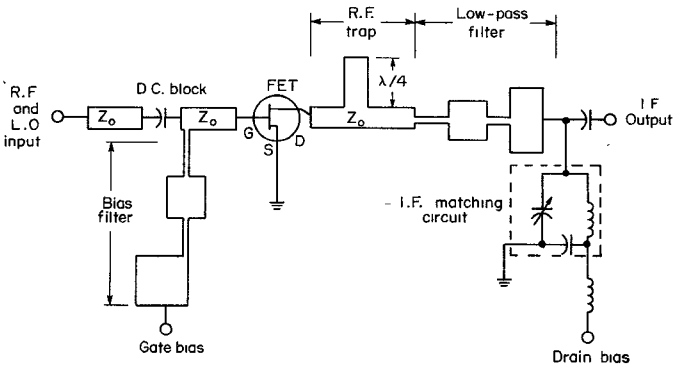

Fig. 7. Circuit configuration of integrated GaAs MESFET mixer used in X-band experiments.

The data shown in Figs. 2, 4–6 pertain to the 71018 series. The second FET, series 40713, has the aforementioned gate width, a gate length of 1.4 μm, a terminal pinchoff voltage of 2.1 V, and a channel doping of 10^{17} cm^{-3}. The f_{max} value of the latter is in the range 25–30 GHz. For the 71018 series it is lower, but was not measured.

All experiments were performed with the mixer circuit in integrated form on a 20-mil-thick alumina substrate. All conductors were gold. The RF frequency was in the vicinity of 8 GHz, the IF frequency was maintained at 30 MHz.

A schematic of the mixer circuit is shown in Fig. 7. The alumina substrate consists of two parts which lie on a common metal base containing a ridge. The ridge divides the base into two contiguous sections. The two alumina wafers butt against the ridge and connect to the gate and drain terminals of the beam-leaded FET chip which is mounted, grounded source, on the ridge. One of the wafers contains the input or RF circuitry which appears to the "left" of the FET in the schematic (Fig. 7). The other wafer contains the IF circuitry. The IF impedance matching network shown in Fig. 7 was made of lumped elements and was contained in a separate chassis because of the low frequency.

The blocking capacitor in series with the RF line was in interdigitated form. The bias filter in the gate circuit provided a low impedance termination at the IF. On the IF side a quarter-wave stub acts as a short-circuit termination for the RF, image, and LO signals. The IF impedance at 30 MHz is high, approximately 1500–2000 Ω. It is matched to 50 Ω by adjustment of the air capacitors in the matching circuit. A low-pass filter precedes the matching circuit.

We have measured only the gain characteristics of the 71018 series to convince ourselves of the validity of the theoretical small-signal model. Following this, we then changed to the higher frequency 40713 series which we also used to measure gain. We then arranged a pair of these single-ended mixers in a balanced configuration to minimize LO-introduced noise. With this balanced mixer configuration we again measured gain and, in addition, the gain compression level, intermodulation products, and noise performance.

A block diagram of the balanced mixer configuration is shown in Fig. 8. Notice the presence of phase shifters in each IF branch. In diode mixers cancellation of the LO-introduced noise can be achieved by reversing the terminals of one of the diodes. Obviously, this cannot be done with FET's. The 180° phase shift between the two IF branches can be accomplished by use of leading and lagging phase shifters as shown in Fig. 8. These phase shifters are constructed of lumped elements and can be incorporated into the IF matching network.

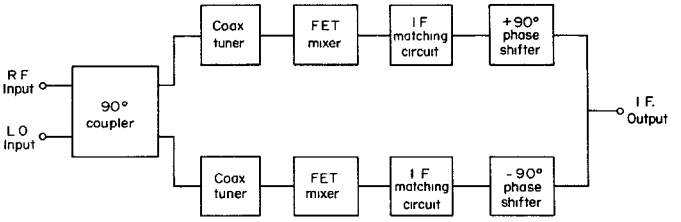

Fig. 8. Block diagram of balanced FET mixer showing phase shifters in output circuit for cancellation of LO noise.

Before we display our results, a brief description will be given of the microwave test setup for measuring the gain and noise figure.

B. Experimental Test Arrangement

The experimental data were obtained with the setup described in Fig. 9. The LO power was supplied by a klystron (X13) capable of delivering up to 80 mW at 8 GHz. The signal generator's output was in excess of +6 dBm. The measurements at the 30-MHz IF frequency were made with an AIL receiver. Because of its narrow bandwidth, we found it necessary to lock the signal 30 MHz away from the LO frequency. A second mixer and a 30-MHz discriminator were used for this purpose.

1) Gain Measurements: The LO and signal power were carefully calibrated with a power meter. The levels could be determined easily with the precision attenuators of the setup. The 30-MHz output power was measured on the receiver, which was calibrated with a separate 30-MHz generator and a power meter. By using a precision IF attenuator at the input, the receiver was kept at a constant level, thus eliminating errors due to nonlinearities.

2) Noise Measurements: The noise figure of the mixer was measured by the so-called Y factor method with the IF precision attenuator and the 30-MHz receiver. The noise source was solid state with an ENR of 15.5 dB, and was broad band. The noise figure is the double channel value.[3]

3) Intermodulation Products: The third-order intermodulation products were measured with the help of an HP 8553B low-frequency spectrum analyzer. The outputs of the two signal generators, 1 MHz apart, were adjusted to have equal amplitude. They were combined and the resultant level adjusted independently. The magnitude of the intermodulation products could be measured directly on the calibrated screen of the analyzer.

For the measurement of gain compression the level of

[3] Simultaneous excitation at signal and image channels.

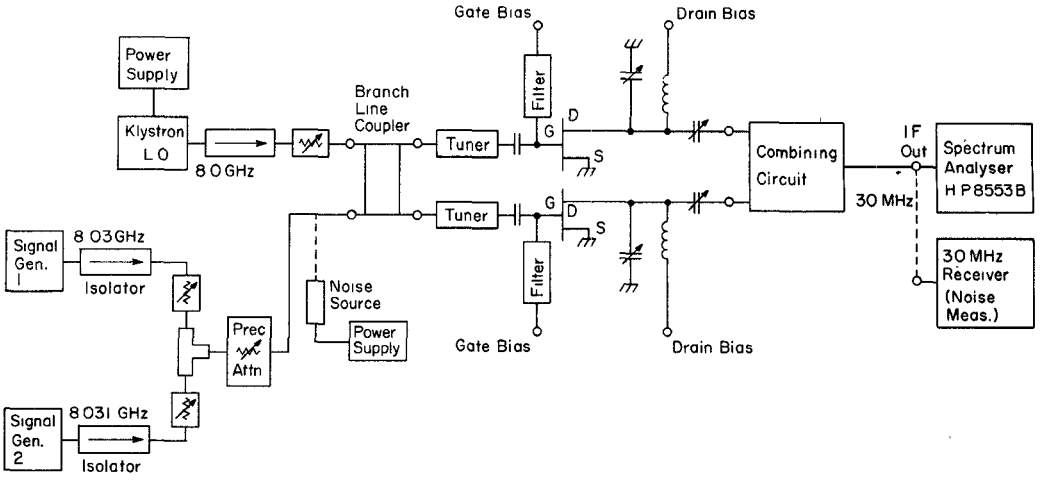

Fig. 9. Test setup for measurement of gain, intermodulation products, and noise figure of GaAs MESFET mixer.

LO power and one signal generator was set, while the other signal level was raised until a decrease of 1 dB was observed at the IF output corresponding to the fixed signal.

4) Corrections: Our results have been corrected to take into account the ohmic losses of the input circuit. The microstrip 3-dB hybrid coupler and the double-stub tuners present losses which attenuate the LO and signal powers and affect the noise figure measurement.

The input circuit was tuned for best operation of the mixer. Its attenuation was determined by measuring the insertion loss of each component separately. The 3-dB directional coupler had an insertion loss of 0.8 dB and the stub tuners 1.2 dB, giving a total loss of 2.0 dB for the input circuit.

The LO and signal powers were corrected by this amount. Thus the gain reported here is the conversion gain of the FET devices.

The noise figure measured includes the noise contributions of the input matching network preceding the mixer and the receiver preamplifier following the mixer. If we attribute the insertion loss of the hybrid coupler and double-stub tuners to dissipation only, then the noise figure of the input circuit is just equal to its insertion loss. Letting the insertion loss be L and the noise figure of the receiver preamplifier be F_r, then by the cascade noise formula the measured noise figure F_m is given by

$$F_m = L + (F - 1)L + \frac{(F_r - 1)L}{G_c} \tag{15}$$

where F is the noise figure of the mixer and G_c is its conversion gain. From the preceding equation, the noise figure of the mixer is

$$F = \frac{F_m}{L} - \frac{F_r - 1}{G_c}. \tag{16}$$

The corrected noise figure F is the one reported here.

C. Conversion Gain

The measured conversion gain as a function of LO power for a 71018 unit is illustrated in Fig. 10 [3]. The device was

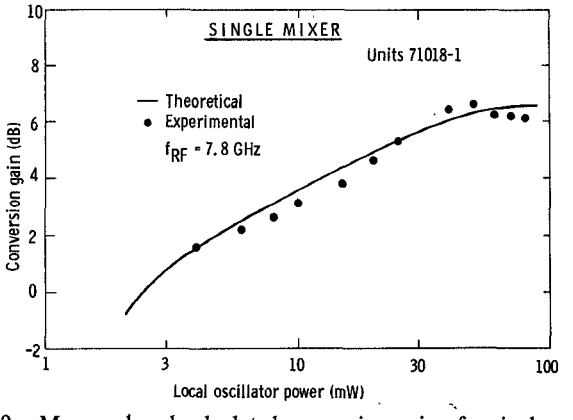

Fig. 10. Measured and calculated conversion gain of a single-ended MESFET mixer showing good agreement between theory and experiment.

operated near pinchoff. Also shown is the theoretical gain calculated by the method described in Section II. Note the excellent agreement. Observe that conversion gain is obtained with a LO drive level as low as 3 mW. It is interesting that the 6.4-dB maximum conversion gain exceeds the maximum linear amplifier gain of 4.7 dB at 7.8 GHz predicted on the basis of the measured S parameters.

The LO power required for maximum conversion gain can be reduced substantially by decrease of the pinchoff voltage. We have verified this with the 40713 series. The measured conversion gain is shown in Fig. 11(a) [4]. Note that nearly the same 6-dB maximum gain is obtained as before, but with approximately 50 percent of the LO power. By a further 50-percent reduction of the LO power to 8 mW, only 1-dB reduction in gain results.

Fig. 11(b) illustrates the excellent signal-handling property of the FET mixer. Note that unlike the diode mixer a higher LO power does not necessarily imply a higher 1-dB gain compression point. Indeed, our measurements indicate that there exists an optimum LO power to give a maximum 1-dB gain compression point. It should be pointed out that the 1-dB gain compression level at the lower LO power

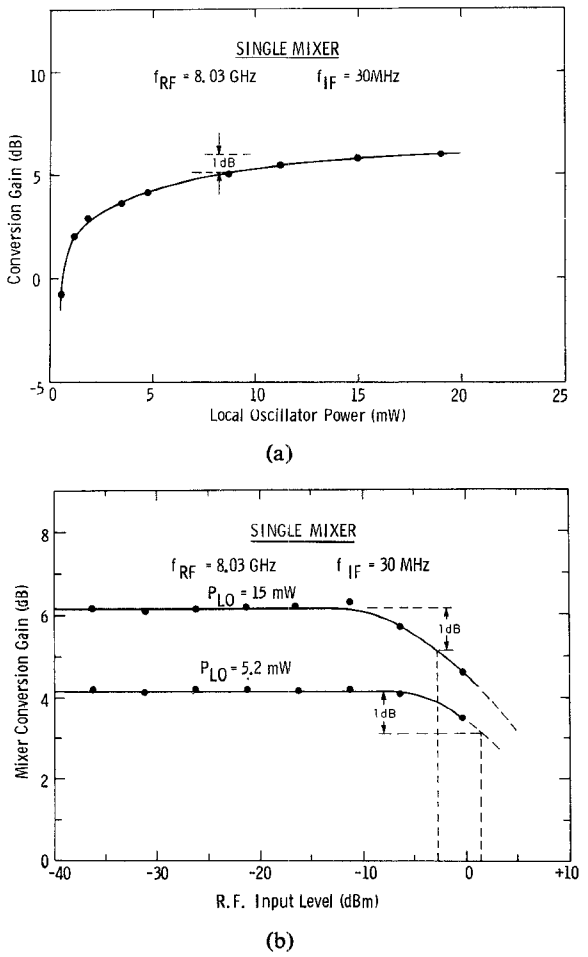

Fig. 11. Measured conversion gain of a GaAs MESFET mixer as a function of (a) LO power and (b) RF input signal level.

occurs at an IF power level exceeding +5 dBm. This is about 10 dB higher than for low-level (Class I) commercially available balanced diode mixers [5].

D. Noise Figure

A balanced mixer was assembled using two separate single mixer modules, and the gain, distortion, and noise characteristics were measured. Correcting for losses in the coaxial tuners and the 90° hybrid coupler (totaling about 2 dB), we obtained the very promising results shown in Fig. 12.

We believe that the minimum noise figure, 7.4 dB, is the lowest reported for an FET mixer operating at this high an RF frequency. Note that at the minimum noise point, the total LO power is only 6 mW, well within the range of an FET oscillator. At this operating point the gain is still in excess of 3 dB, nearly 10 dB higher than for a diode mixer—thus eliminating the need of a preamplifier.

The mild dependence of the noise figure on LO power suggests that there may be a considerable 30-MHz component of $1/f$ base-band noise being amplified. There is some evidence that this noise can be reduced considerably by using a high-resistivity buffer layer between the channel epitaxial layer and the substrate interface. For example, noise figures of buffered-layer FET amplifiers show a significant improvement in noise performance [1]. Sitch and Robson have also obtained appreciable noise reduction with buffered-layer FET mixers operating at S band [6].

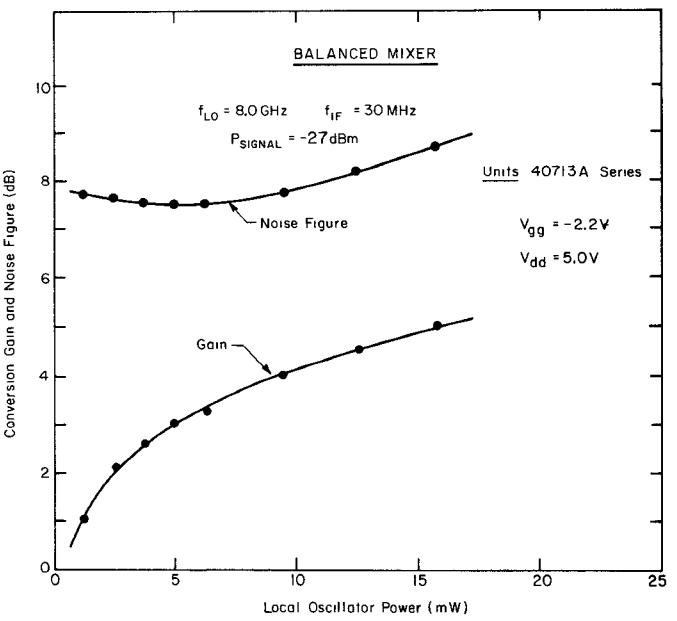

Fig. 12. Measured conversion gain and double channel noise figure of a balanced GaAs MESFET mixer at X band as a function of LO drive.

Noise degradation by the LO source also is possible because of a mismatch in either the conversion gain or phase shift of the two single-ended mixers. To eliminate this possibility, we have analyzed the noise contribution of the LO source.

Let $(N/C)_{dsb}$ denote the double side-band AM noise-to-carrier ratio of the LO in a band B, 30 MHz from the carrier as seen by the mixer. If P_{0t} is the total LO power delivered to the balanced mixer gate terminals, then the degradation in the noise figure attributable to a phase imbalance $\Delta\phi$ in the two mixer IF ports is

$$\Delta F_{\phi} = \left(\frac{N}{C}\right)_{dsb} \frac{P_{0t}}{kT_0B} (\tan \Delta\phi/2)^2 \tag{17}$$

where $k = 1.38 \times 10^{-23}$ J/K and $T_0 = 290$ K. We define the phase imbalance as $\Delta\phi = 180° - |\phi_1 - \phi_2|$, where ϕ_1 and ϕ_2 are the phase shifts in either IF arm, with due regard for algebraic sign. Expression (17) does not include gain imbalance.

The degradation from gain imbalance is expressible as

$$\Delta F_g = \left[\frac{\sqrt{\frac{G_2}{G_1}} - 1}{\sqrt{\frac{G_2}{G_1}} + 1}\right]^2 \left(\frac{N}{C}\right)_{dsb} \frac{P_{0t}}{2kT_0B}. \tag{18}$$

The measured phase imbalance of the phase-shifting network in a 10-MHz band centered at 30 MHz was less than 12°. The gain imbalance was approximately 1 dB. The measured $(N/C)_{dsb} = -179$ dB in a 1-Hz band. For a total oscillator power of 6 mW (the value of the noise minimum

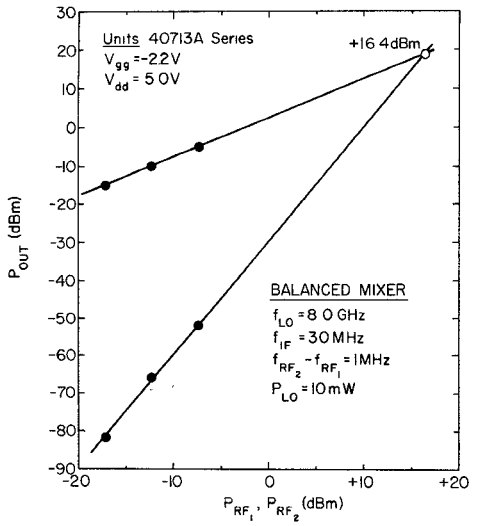

Fig. 13. Third-order two-tone modulation curves obtained with balanced GaAs MESFET mixer at X band.

Mixer	Maximum gain	Minimum noise figure	Output * 3rd-order IM intercept	Output 1dB gain compression level
GaAs FET	+6dB	7.4 dB	+20dBm	+5.5 dBm
Diode † (low-level)	-5dB	5-7 dB	+5 dBm	-6 to -1dBm

* at P_{LO} = +8dBm † Cheadle, MICROWAVES (Dec.1973)

Fig. 14. Table comparing noise performance and signal-handling capabilities of the GaAs MESFET mixer and low-level diode mixer.

in Fig. 11), the calculated degradation in the mixer noise figure is $\Delta F_\phi = 2.1 \times 10^{-2}$ for the phase imbalance and $\Delta F_g = 3.1 \times 10^{-3}$ for the gain imbalance. Therefore the increase in the noise figure at the minimum is only 0.02 dB, a negligible quantity.

E. Intermodulation Distortion

Fig. 13 displays our results obtained in a two-tone intermodulation experiment. Note that the intersection corresponds to a third-order intermodulation level of +16.4 dBm at the input to the mixer, or +20 dBm at the IF output! These values are consistent with those reported by Sitch and Robson for an S-band GaAs MESFET mixer [6]. By comparison the output IM point typical of low-level balanced diode mixers is in the range of −6 to −1 dBm, over 10 dB lower. Furthermore, the output level corresponding to the 1-dB gain compression point is also some 10 dB lower than for the FET mixer.

Fig. 14 is a table comparing the signal-handling capabilities and noise performance of the GaAs FET and the low-level diode mixer. It is apparent that even at this stage of development the GaAs MESFET mixer has nearly a 10-dB advantage over the diode mixer in the gain and in the signal distortion levels. The small difference in the noise figure, we believe, will narrow in the near future, and possibly change sign.

F. Burn-Out Level

We have not performed burn-out tests on the GaAs MESFET mixer. However, such tests were made on similar FET's in amplifier circuits. CW power levels in excess of 1 W were impressed on the gate without permanent damage.

V. Summary

We have shown that the GaAs MESFET mixer can exhibit conversion gain at microwave frequencies, which is predictable from a simple circuit model based on the small-signal properties of the FET and the modulation characteristics of the low-frequency transconductance.

The experimental results show that the GaAs MESFET is a promising candidate for integrated front-end applications at X band, and possibly at higher frequencies.

A substantial improvement in the noise properties is expected with the use of buffered-layer devices, so that the GaAs MESFET mixer may become competitive and perhaps superior to existing solid-state devices operating with comparable signal levels.

Appendix
Derivation of Expression for Conversion Gain

We shall derive the expression for $I_6/E_1 = -\Delta/\Delta_z$ which appears in the gain expression (6a). For convenience let $Z_{kk} + Z_k = Z_{kk}'$. The determinant Δ_z is given by

$$\Delta_z = \begin{vmatrix} Z_{11}'^* & 0 & 0 & Z_{14}^* & 0 & 0 \\ 0 & Z_{22}' & 0 & 0 & Z_{25} & 0 \\ 0 & 0 & Z_{33}' & 0 & 0 & Z_{36} \\ Z_{41}^* & 0 & Z_{43} & Z_{44}'^* & 0 & 0 \\ 0 & Z_{52} & Z_{53} & 0 & Z_{55}' & 0 \\ Z_{61}^* & Z_{62} & Z_{63} & 0 & 0 & Z_{66}' \end{vmatrix} \tag{A1}$$

and Δ is obtained from Δ_z by deleting the first row and sixth column.

We now assume that $\bar{R}_d \gg R_s$, R_{dr}, and $g_0 R_s \ll 1$, both of which are true for well-designed GaAs MESFET's. Then one may show that

$$\frac{I_6}{E_1} = +j\left(\frac{g_1 \bar{R}_d}{\omega_1 \bar{C}}\right) \frac{1}{(Z_{11}^* + Z_1^*)(Z_{66} + Z_6) + \delta} \tag{A2}$$

where δ is given by

$$\delta = \frac{1}{\omega_3}\left(\frac{g_1 R_s \bar{R}_d}{\bar{C}}\right)^2 \frac{\omega_2^{-1}(Z_{11}^* + Z_1^*)(Z_{44}^* + Z_4^*) - \omega_1^{-1}(Z_{22} + Z_2)(Z_{55} + Z_5)}{(Z_{22} + Z_2)(Z_{33} + Z_3)(Z_{44}^* + Z_4^*)(Z_{55} + Z_5)}. \tag{A3}$$

Notice that the first term in the denominator of (A2) involves only the input RF circuit and the output IF circuit. The terminations at the remaining ports only enter in δ.

When $\omega_3 \ll \omega_1$ the image loop impedances can be approximated by the first two terms of the Taylor expansion

of the signal impedances,

$$Z_{22} + Z_2 = Z_{11} + Z_1 + 2\frac{\partial(Z_{11} + Z_1)}{\partial\omega_1}\omega_3 + \cdots \tag{A4}$$

$$Z_{55} + Z_5 = Z_{44} + Z_4 + 2\frac{\partial(Z_{55} + Z_5)}{\partial\omega_1}\omega_3 + \cdots. \tag{A5}$$

Inserting these expansions into (A3), noting that $\omega_2^{-1} \cong \omega_{-1}(1 - 2\omega_3/\omega_1)$ and $Z_{33} + Z_3 \sim 1/\omega_3\bar{C}$, one obtains, after neglecting all terms of order ω_3/ω_1, the result

$$\delta = \frac{(g_1 R_s \bar{R}_d)^2}{\omega_1 \bar{C}} \mathrm{O}\left[\frac{1}{(Z_{44} + Z_4)}\right] \tag{A6}$$

where the symbol O denotes "the order of" the argument in parentheses. But $Z_{44} + Z_4 \geq \bar{R}_d$, so

$$\delta < (g_1 R_s)^2 \frac{\bar{R}_d}{\omega_1 \bar{C}}.$$

To compare δ with the first term in the denominator of (A2), we note that

$$(Z_{11} + Z_1)^*(Z_{66} + Z_6) = \mathrm{O}(R_{\mathrm{in}}\bar{R}_d).$$

Thus the ratio of δ to this term is of the order of $(g_1 R_s)^2/\omega_1\bar{C}R_{\mathrm{in}}$. Since $\omega_1\bar{C}R_{\mathrm{in}} = \mathrm{O}(0.5)$ for a well-designed FET, whereas $g_1 R_s = \mathrm{O}(0.05)$, the δ term in the denominator of (A2) is less than 1 percent of the first term and can be neglected. Thus the terminations at the ports other than the signal input and IF output are not of critical importance. Therefore the available conversion gain is given to good accuracy by

$$G_{\mathrm{av}} = 4R_g R_L \left(\frac{g_1\bar{R}_d}{\omega_1\bar{C}}\right)^2 \frac{1}{|Z_{11} + Z_1|^2|Z_{66} + Z_6|^2} \tag{A7a}$$

$$= \left(\frac{2g_1\bar{R}_d}{\omega_1\bar{C}}\right)^2 \frac{R_g R_L}{|Z_{11} + Z_1|^2|Z_{66} + Z_6|^2}. \tag{A7b}$$

When the substitutions $Z_1 = Z_g = R_g + jX_g$, $Z_6 = R_L + jX_L$, $Z_{66} = \bar{R}_d$, and $Z_{11} = R_{\mathrm{in}} + (j\omega_1\bar{C})^{-1}$ are made, (7) of the text is obtained.

Acknowledgment

The authors wish to thank Dr. C. F. Krumm for fabricating the excellent beam-lead devices, S. R. Steele for the high-quality epitaxial material, and R. W. Bierig for his constant encouragement throughout this study.

References

[1] R. A. Pucel, D. Massé, and C. F. Krumm, "Noise performance of gallium arsenide field-effect transistors," *Proc. Fifth Biennial Cornell Electrical Engineering Conf.*, Cornell University, 1975.

[2] R. A. Pucel, H. A. Haus, and H. Statz, *Advances in Electronics and Electron Physics 38*, "Signal and noise properties of gallium arsenide field-effect transistors." New York: Academic, 1975, pp. 195–265.

[3] R. A. Pucel, R. Bera, and D. Massé, "An evaluation of GaAs FET oscillators and mixers for integrated front-end applications," *Digest of Technical Papers, 1975 IEEE Int. Solid-State Circuits Conf.*, Philadelphia, PA, pp. 62–63.

[4] R. A. Pucel, D. Massé, and R. Bera, "Integrated GaAs FET mixer performance at *X*-band," *Electronics Letters*, vol. 11, no. 9, pp. 199–200, May 1, 1975.

[5] D. Cheadle, "Selecting mixers for best intermodulation performance," *Microwaves*, Part I, pp. 48–52, Nov. 1973; Part II, pp. 58–62, Dec. 1973.

[6] J. E. Sitch and P. N. Robson, "The performance of GaAs field-effect transistors as microwave mixers," *Proc. IEEE*, vol. 61, pp. 399–400, Mar. 1973.